

# Supplementary Material: Ultra-fast X-ray Diffraction Studies of the Phase Transitions and Equation of State of Scandium Shock-Compressed to 82 GPa

R. Briggs,<sup>1</sup> M.G. Gorman,<sup>1</sup> A.L. Coleman,<sup>1</sup> R.S. McWilliams,<sup>1</sup> E.E. McBride,<sup>2</sup> D. McGonegle,<sup>3</sup> L. Peacock,<sup>4</sup> S. Rothman,<sup>4</sup> S.G. Macleod,<sup>4,5</sup> C.A. Bolme,<sup>6</sup> A.E. Gleason,<sup>6</sup> G.W. Collins,<sup>7</sup> J.H. Eggert,<sup>7</sup> D.E. Fratanduono,<sup>7</sup> R.F. Smith,<sup>7</sup> E. Galtier,<sup>8</sup> E. Granados,<sup>8</sup> H.J. Lee,<sup>8</sup> B. Nagler,<sup>8</sup> I. Nam,<sup>8</sup> Z. Xing,<sup>8</sup> J.S. Wark,<sup>3</sup> and M.I. McMahon<sup>1,5</sup>

<sup>1</sup>*SUPA, School of Physics and Astronomy, and Centre for Science at Extreme Conditions, The University of Edinburgh, Mayfield Road, Edinburgh, EH9 3JZ, UK.*

<sup>2</sup>*European XFEL, Albert-Einstein-Ring 19, D-22761 Hamburg, Germany*

<sup>3</sup>*Department of Physics, Clarendon Laboratory, Parks Road, University of Oxford, Oxford OX1 3PU, UK*

<sup>4</sup>*Atomic Weapons Establishment, Aldermaston, Reading, RG7 4PR, United Kingdom*

<sup>5</sup>*Research Complex at Harwell, Didcot, Oxon, OX11 0FA, United Kingdom*

<sup>6</sup>*Shock and Detonation Physics, Los Alamos National Laboratory, PO Box 1663, Los Alamos, New Mexico 87545, USA*

<sup>7</sup>*Lawrence Livermore National Laboratory, 6000 East Avenue, Livermore, California 94500, USA*

<sup>8</sup>*Linac Coherent Light Source, SLAC National Accelerator Laboratory, Menlo Park, California 94025, USA*

(Dated: October 18, 2016)

PACS numbers: 61.50.Ks, 62.50.+p

## LCLS EXPERIMENTAL PROCEDURE

Scandium foils 25(5)  $\mu\text{m}$  thick (Goodfellow, 99 % purity) were cut into  $3 \times 3 \text{ mm}^2$  targets and, following individual thickness measurements to an accuracy of 0.1  $\mu\text{m}$ , were glued to a 50  $\mu\text{m}$  thick polyimide ablator. The texture of the as-purchased Sc foil was characterized prior to the LCLS experiment using synchrotron radiation, and the targets were all mounted on the MEC beamline such that the arc of maximum intensity of the highly-textured (002) Debye-Scherrer ring in the ambient-pressure hcp-Sc diffraction pattern was observed centrally on the main CSPAD detector (see Figure 1 in the main paper). The targets were mounted in a holder which held up to 240 targets, the maximum number of shots achievable in a 12-hour experimental shift. In some of the targets a LiF optical window was used. These were 100  $\mu\text{m}$  thick and had a 100 nm thick Al coating on the face that was glued to the normally-free surface. The pressure within the Sc sample was established from the value measured in the LiF by impedance matching using prior Sc shock data.

Alignment crystals (Yttrium Aluminium Garnet) and X-ray diffraction calibrants ( $\text{CeO}_2$ ,  $\text{MoO}_3$  and  $\text{LaB}_6$ ) were also inserted into the target holder. The YAG crystals were used to align the drive lasers via fluorescence. The focused X-ray beam, which was incident at  $18^\circ$  to the target normal, was centered on the drive laser spot such that diffraction was always collected at the center of the driven region. Diffraction patterns from the X-ray calibrants were obtained before and during each experimental shift from which the positions and angles of each of the CSPAD detectors were determined. For each driven target, the laser pulse shape was measured using a fast oscilloscope.

The rear free surface velocity of the Sc targets during each laser drive was measured as a function of time using

a velocity interferometer (VISAR) [1]. The free surface velocity was compared to existing data in the literature for Sc and, using the  $2u_p$  approximation to obtain particle velocity, and the sample density obtained from the diffraction data, the pressure of the shocked sample was obtained. Figure S1 shows raw VISAR data (top), which shows the planarity of the laser drive across the sample region probed by the X-ray beam (as determined from the variation in the breakout time) to be 5%, and the free surface velocity extracted from the VISAR data using the fast Fourier transform method (FFT) (bottom).

Uncertainties in the pressure arise from variations in the particle velocity within the compressed region of the sample at the time of data collection, as estimated from the observed time history of the free-surface velocity (typically  $\sim 3\%$ ) recorded by the two VISARS, and uncertainties in the density (typically  $\sim 1\%$ ), as determined from the unit cell parameters obtained by profile fitting, or fitting to measured d-spacings. The uncertainty in shock speed ( $\sim 4\%$ ) and pressure ( $\sim 7\%$ ) are then obtained by propagating the uncertainties through the Rankine-Hugoniot equations.

The 2D diffraction images recorded on the different CSPAD detectors were integrated azimuthally using a MATLAB code and the resulting profiles were analysed using both profile refinement (Rietveld) techniques, and by least-squares analysis of the positions of individual Bragg peaks.

## GRAIN SIZE AND STRAIN ANALYSIS

The average grain size and microstrain in the sample can be estimated using a modified Warren-Averbach (WA) analysis of the X-ray diffraction peak widths [3–5]. The X-ray diffraction peaks are fitted with a Gaussian

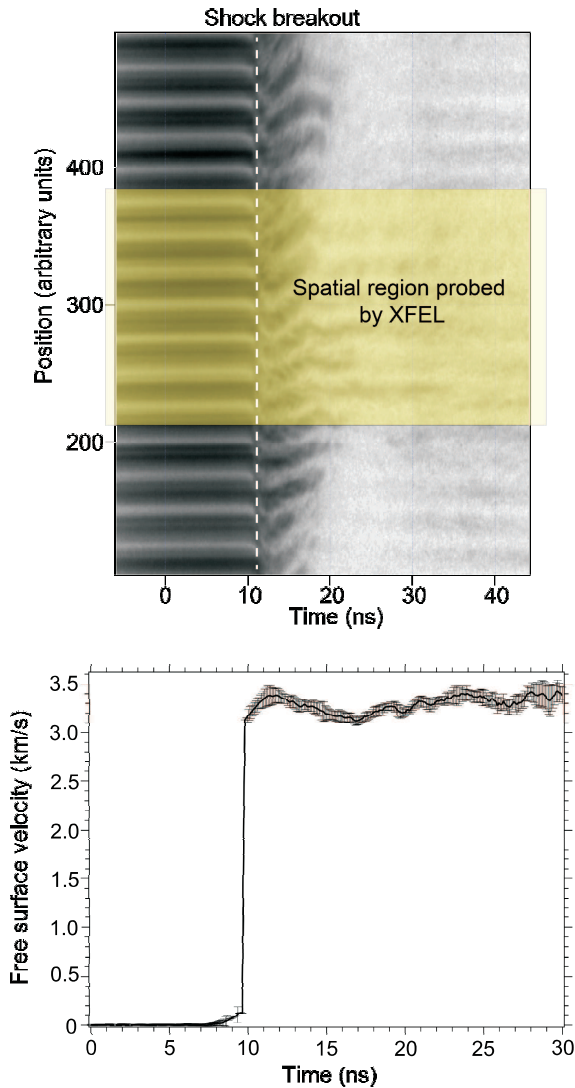


FIG. S1: Top: A typical VISAR image from one of the streak cameras. The yellow shaded area shows the region of the sample illuminated by the  $50 \times 50 \mu\text{m}^2$  X-ray beam. Bottom: The corresponding free surface velocity trace, which is extracted from the raw data using the fast Fourier transform method (FFT). The standard deviations of velocity over the analyzed region are included, and the trace shows a peak free surface velocity of 3.35 km/s. Using the acoustic approximation, where the particle velocity is half that of the free surface velocity [2], the peak particle velocity is 1.675 km/s, which, combined with a  $V/V_0$  value of 0.739(2) obtained from the lattice parameter of bcc-Sc, corresponds to a peak pressure of 32.0 GPa along the Principal Hugoniot.

distribution function such that a single diffraction peak can be described by

$$a(hkl) = \exp(-g^2/W^2) \quad (1)$$

where  $g$  is the scattering vector of the lattice plane ( $hkl$ ). By plotting the square of the peak width ( $W^2$ )

against the square of the inverse scattering vector ( $Q_{hkl}^2$ ) (see Figure S2) one can obtain the grain size from the relation:

$$W^2 = B^2 + A^2 Q_{hkl}^2 \quad (2)$$

where the intercept is related to the grain size,  $\sigma$ , by ( $B = 2\pi/\sigma$ ), and the gradient is related to the r.m.s. strain,  $\sqrt{\langle \varepsilon^2 \rangle}$ , by  $A = 2\sqrt{2}\pi\sqrt{\langle \varepsilon^2 \rangle}$ .

Using the CeO<sub>2</sub> NIST standard material 674b, with a measured grain size of  $380.6 \pm 4.5$  nm [6], the instrumental broadening in  $2\theta$  was found to be  $\sim 0.6^\circ$ , the same value previously reported by Gleason *et al.* [5] for the same instrument. Applying the WA analysis to the uncompressed Sc diffraction peaks (after taking the instrumental broadening into account) gave a grain size of 85(17) nm for the ambient as-purchased Sc foil (Figure S2). An estimation of the grain size for the shock compressed material was applied to the hcp-Sc data at 19.5 GPa, where we could accurately determine the widths of the higher-Q diffraction peaks required for the WA analysis. The grain size of hcp-Sc at 19.5 GPa was 25(3) nm, with an r.m.s. strain of  $< 0.2$  %.

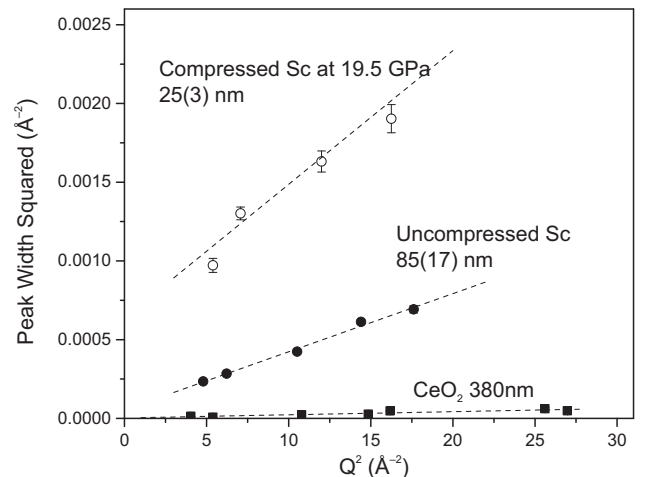


FIG. S2: Plot of the peak widths squared versus  $Q^2$ , as used to determine the grain size for the CeO<sub>2</sub> standard, the uncompressed Sc foil and compressed hcp-Sc at 19.5 GPa. The dashed lines are least-squares linear fits to the data points.

## DIAMOND EXPERIMENTAL PROCEDURE

Diffraction data from Sc compressed in a resistively-heated diamond anvil cell (DAC) were obtained up to 30 GPa and 900 K. The sample was cut from the same 25  $\mu\text{m}$  Sc foil used in the LCLS experiments, and was loaded with a small piece of Cu foil as a pressure calibrant. No pressure transmitting medium was used. Diffraction data were collected on beamline I15 at the Diamond

Light Source using an x-ray wavelength of  $0.4246\text{\AA}$  and a beam size of  $20\ \mu\text{m}$ . The diffraction data were collected on a mar345 image-plate detector placed approximately 380 mm from the sample, and the two-dimensional (2D) diffraction images were integrated using FIT2D [7] to give standard diffraction profiles. Diffraction data were collected from two different samples in a series of isothermal pressure scans at 413 K, 623 K and 848 K. Attempts to collect data at still higher temperatures were unsuccessful as the sample reacted with the diamonds and/or rhenium gasket. The hcp to host-guest (HG) transition was observed clearly at all three temperatures, and the host-guest phase was found to be ordered in each case. The order-disorder transition in the guest chains thus takes place between 848 K and  $\sim 1700\text{ K}$ , the lowest temperature at which the HG phase was observed along the Hugoniot.

### PRESSURE ESTIMATE FOR LIQUID-ONLY DATA AT $\sim 82\text{ GPa}$

Diffraction data collected using the highest-available drive laser intensity revealed only scattering from liquid-Sc, along with diffraction peaks from uncompressed hcp-Sc (see profile (vii) in Figure 1). Unfortunately, the sample became completely non-reflecting for this shot and the VISAR diagnostic recorded no fringes. The pressure could not be determined using the VISAR therefore. However, from diffraction data collected from liquid-Sc at ambient pressure, obtained after the pressure had fully released, and from three liquid-Sc diffraction patterns obtained near 60 GPa, where the pressure could be determined by VISAR, we could estimate the pressure dependence of position of the main liquid diffraction peak. A simple linear extrapolation of this pressure-dependence (see Figure S3), combined with the measured position of the liquid-diffraction peak in the highest-pressure shot, allowed us to estimate the pressure of the liquid-only sample as 82 GPa. While the uncertainty on this value is quite large, we estimate  $\pm 5\text{ GPa}$ , the sample pressure is certainly higher than 72 GPa, the highest pressure measured with the VISAR, and where the position of the diffraction peak from the liquid-Sc was clearly at a lower angle (the exact position of the liquid diffraction peak at 72 GPa could not be determined, as it is overlapped by the strongest Bragg peaks from the HG phase).

### RIETVELD FIT TO SC AT 35 GPa

The two-phase Rietveld fit to the bcc-Sc profile obtained at 35 GPa is shown in Figure S4.

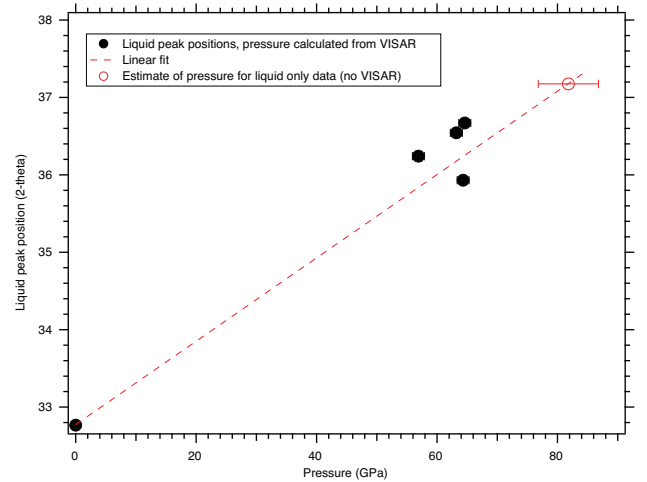


FIG. S3: The pressure dependence of the position of the most intense diffraction peak in liquid-Sc. Extrapolation of the peak positions and pressure determined from VISAR measurements (filled circles) was used to estimate the pressure of the liquid-only sample (open circle).

### ACCURACY OF EQUATION OF STATE DATA

Shock Hugoniot conditions were determined via a quasi-absolute equation-of-state measurement based on the volumes determined from diffraction and free surface velocities determined by VISAR. The unit cell volume is known to high accuracy, and we assume that the volume measured by diffraction represents the specific volume of the bulk sample, which is exactly true where the shocked state is a single phase. Maximum deviations from this assumption for the mixed HG-liquid phase region can be estimated based on the density difference between the coexisting liquid and solid inferred from our phase diagram. The ambient latent heat of melting ( $16\text{ kJ/mol}$ ) and melting temperature ( $1812\text{ K}$ ) [10] imply an entropy difference of  $8.8\text{ J/mol/K}$ . Assuming this remains constant under pressure, the Clapeyron slope near shock melting ( $5.5\text{ K/GPa}$ ), see Figure 5, implies a density difference of  $\sim 0.5\%$  between solid and liquid. Our data in this region fall toward the liquid-rich end of the coexistence region (Fig. 5), such that liquid should represent just over 50% of the bulk. Thus, in the linear mixing approximation, the bulk density should differ by no more than 0.3-0.4% from that measured in the HG subsystem. As our errors are already of order 1%, this plausible systematic error is considered to be satisfactorily included within our error bars.

Another source of systematic error that might be present in this EoS measurement is associated with the assumption of symmetric release at the free surface to produce a free surface velocity of twice the particle speed. However, this has been found for metals at modest pressures to be an excellent approximation, even in cases

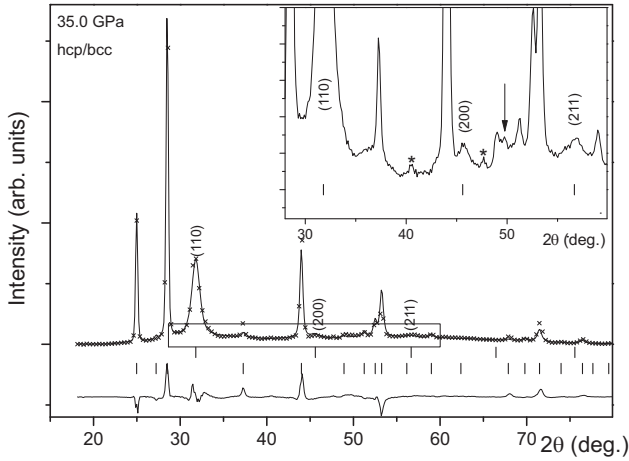


FIG. S4: A two-phase (50%:50% uncompressed-hcp:bcc) Rietveld fit to the diffraction profile obtained at 35.0 GPa ( $\lambda=1.240\text{\AA}$ ), with the most intense bcc peaks indexed. The calculated peak positions of the best-fitting uncompressed-hcp and bcc unit cells are shown by the lower and upper tick marks beneath the profile. The inset shows an enlarged view of observed diffraction profile, highlighting the weaker bcc peaks, whose calculated positions are shown by the tick marks. The origin of the two extremely weak peaks marked with asterisks is unknown. They are too sharp to come from the compressed sample, and may come from material ablated off neighbouring targets in previous shots. The feature identified with an arrow is a detector-edge effect.

where phase transitions occur, so long as wave profiles are measured with sufficient detail and precision [11, 12]. In the present study, we observe no evidence for multiple-wave structure at the free-surface originating from the phase transitions, so interpretation of free-surface velocities is straightforward. A plausible systematic error of 2% in our determination of  $u_p$  is suggested considering typical errors in this approximation [11]. As this is similar to, or smaller than, measurement uncertainty, it is considered to be accounted for.

### THE ROOM TEMPERATURE COMPRESSIBILITY OF HG-SC

The compressibility of HG-Sc at 300 K has been reported by Fujihisa *et al* up to 100 GPa [13]. However, in that study the value of the incommensurate wavevector  $\gamma$ , the ratio of the lengths of the  $c$ -axes of the host and guest substructures, was determined incorrectly. As the number of atoms in the unit cell of the host structure is  $8+(2\times\gamma)$ , then the density of HG-Sc was also determined incorrectly in that study. Using the data provided in Figs. 3 and 4 of Fujihisa *et al* we have determined the volume of the host unit cell, and then recalculated the density up to 100 GPa assuming  $\gamma=1.280$ , the value determined at 23 GPa [14], and that this value is pres-

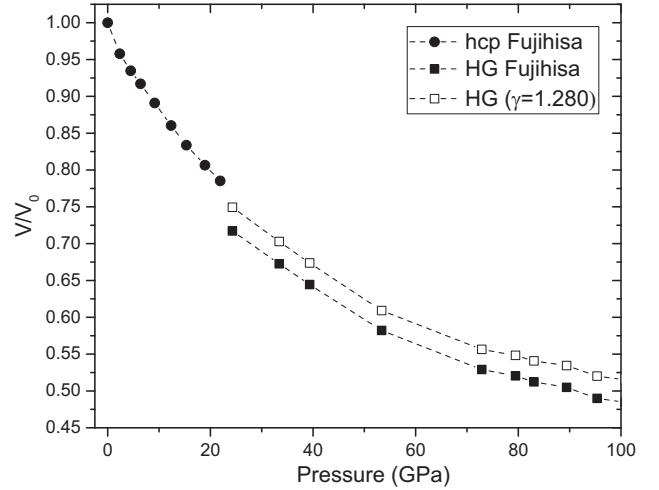


FIG. S5: The isothermal compressibility of the hcp and HG phases of Sc at 300 K. The data reported by Fujihisa *et al* [13] are plotted using solid symbols, while the corrected data for the HG phase, which assume that  $\gamma=1.280$  [14] at all pressures, are plotted using unfilled symbols.

sure independent. The effect on the calculated density is shown in Figure S5. The effect of pressure, temperature and the order-disorder transition on the correct value of  $\gamma$  is unknown.

- [1] P. M. Celliers, D. K. Bradley, G. W. Collins, D. G. Hicks, T. R. Boehly, and W. J. Armstrong, *Review of Scientific Instruments* **75**, 4916 (2004).
- [2] J. W. Forbes, *Shockwave Compression of Condensed Matter* (Springer, 2012).
- [3] B. Warren and B. Averbach, *J. Appl. Phys.* **21**, 595 (1950).
- [4] J. Hawreliak, D. Kalantar, J. Stolken, B. Remington, H. Lorenzana, and J.S. Wark, *Phys. Rev. B* **78**, 220101 (2008).
- [5] A.E. Gleason, C.A. Bolme, H.J. Lee, B. Nagler, E. Galtier, D. Milathianaki, J. Hawreliak, R.G. Kraus, J.H. Eggert, D.E. Fratanduono, G.W. Collins, R. Sandberg, W. Yang and W.L. Mao, *Nature Communications* **6**, 8191 (2015).
- [6] <https://www-s.nist.gov/srmors/certificates/674b.pdf>
- [7] A.P. Hammersley, S.O. Svensson, M. Hanfland, A.N. Fitch, and D.Häusermann, *High Press. Res.* **14**, 235 (1996).
- [8] D. Kammler, M. Rodriguez, R. Tissot, D. Brown, B. Clausen, and T. Sisneros, *Metallurgical and Materials Transactions A* **39**, 2815 (2008).
- [9] Y. Akahama, H. Fujihisa, and H. Kawamura, *Physical Review Letters* **94**, 195503 (2005).
- [10] B. Beaudry and A. Daane, *Transactions of the Metallurgical Society of AIME* **224**, 770 (1962).
- [11] L. M. Barker and R. E. Hollenbach, *Journal of Applied Physics* **45**, 4872 (1974).
- [12] P. M. Celliers, G. W. Collins, D. G. Hicks, and J. H.

- Eggert, Journal of Applied Physics **98**, 113529 (2005).
- [13] H. Fujihisa, Y. Akahama, H. Kawamura, Y. Gotoh, H. Yamawaki, M. Sakashita, S. Takeya, and K. Honda, Physical Review B **72** 132103 (2005), ISSN 1098-0121.
- [14] M. I. McMahon, L. F. Lundegaard, C. Hejny, S. Falconi, and R. J. Nelmes, Physical Review B **73** 134102 (2006).